Environmental Science & Technology

pubs.acs.org/est

Article

Radiological Analyses of ^{226}Ra and ^{238}U in Surface Water and Sediments from the Jackpile Member of the Morrison Formation, Pueblo of Laguna, New Mexico

Virginia G. Rodriguez, Ashabari Majumdar, Isabel Meza, Loretta Corcoran, Amanda Pierson, Kaelin Gagnon, Caitlyn Cano, Abdul-Mehdi S. Ali, Christopher M. Shuey, Gregory Jojola, Wanpeng Tan, Ani Aprahamian, José M. Cerrato, and Peter C. Burns*

Cite This: *Environ. Sci. Technol.* 2024, 58, 15138−15146

Read Online

ACCESS | Metrics & More | Article Recommendations | Supporting Information

ABSTRACT: Surface water and sediments from the Jackpile mine, St. Anthony mine, Rio Paguate, Rio Moquino, and Mesita Dam areas near Pueblo of Laguna, New Mexico, were analyzed for ^{226}Ra and U using gamma (γ) spectroscopy and inductively coupled plasma mass spectroscopy, respectively. Activity ratios for ^{226}Ra/^{238}U for solid samples range from 0.34 ± 0.13 to 16 ± 2.9, which reflect uranium transport and accumulation (<1), relatively pristine material in secular equilibrium (1), and removal of uranium by weathering (>1). Concentrations ranging from 80 to 225 μg L^{-1} U were detected in unfiltered water samples near the Jackpile mine. Water samples upstream and downstream from the mine contained concentrations ranging from 12 to 15 μg L^{-1} U. Water samples collected from the North Pit standing pond in the Jackpile mine contained as much as 1560 pCi L^{-1} of ^{226}Ra, and passing the water through a 0.2 μM filter did not substantially reduce the activity of ^{226}Ra in the water. ^{234}Th and ^{226}Ra are in secular equilibrium in this water, while radon gas was lost from the water. The results of the current study provide insight into the distribution of U-series radionuclides in the Pueblo of Laguna area, including detection of high levels of radioactivity in water at some locations within the Jackpile mine.

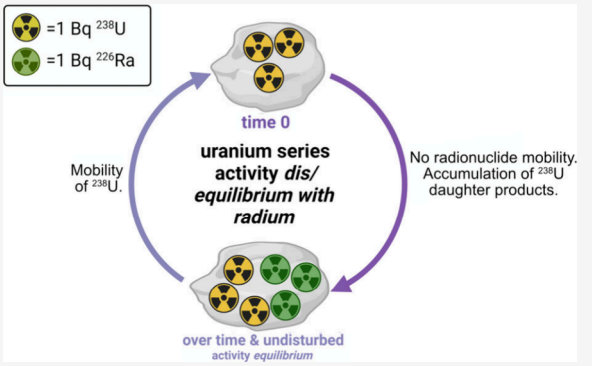

KEYWORDS: *Uranium, radium, uranium mine, legacy site, gamma spectroscopy*

INTRODUCTION

The mining of uranium at many sites throughout the United States has impacted surrounding areas in part due to exposure of mine workings and wastes to weathering and oxidizing conditions.[1−3] Substantial research has been focused on uranium mobility, but much less emphasis has been placed on the environmental fate of its daughters. The decay series of ^{238}U, which has a natural isotopic abundance of 99.27% and a half-life of 4.5 billion years, includes ^{226}Ra, which has a half-life of 1600 years. In a closed system that is sufficiently old, the activity of these two radionuclides will be the same.[4] Uranium-series disequilibrium occurs (the activity ratio of ^{226}Ra and ^{238}U depart from one) if chemical fractionation takes place.[5,6] Transport of radionuclides in the environment is the primary cause of disequilibrium.[7−10]

When ^{226}Ra decays, it emits an α particle and produces ^{222}Rn, which is a relatively short-lived (half-life of 3.8 days) radioactive gas.[11] The radiation from ^{226}Ra, and particularly its decay into radon gas, are concerns for people living near uranium-bearing areas. The geochemical properties of uranium and radium differ radically. Uranium is an actinide that occurs in the tetravalent and hexavalent oxidation states (and rarely in the pentavalent state), and U(VI) forms the water-soluble uranyl ion UO_2^{2+}. The uranyl ion tends to be environmentally mobile.[12] Radium is a large alkali earth divalent cation that is typically immobile in environmentally relevant systems.[7,13] In an oxidizing environment, uranium is transported in water as the dissolved uranyl ion and its complexes, whereas radium is much less soluble. However, environmental concentrations of radium are extremely low.

In a system at secular equilibrium, the activities of ^{238}U and ^{226}Ra will be the same but their elemental concentrations will be vastly different. The specific activity (the number of radioactive transformations per second) of ^{226}Ra is one Ci g^{-1} and that of ^{238}U is 3.364×10^{-7} Ci g^{-1}. A sample in which ^{238}U

Received: February 20, 2024
Revised: July 29, 2024
Accepted: July 30, 2024
Published: August 13, 2024

and ^{226}Ra are in secular equilibrium will have a ^{226}Ra elemental concentration roughly 7 orders of magnitude less than that of ^{238}U.

The Jackpile member of the Morrison Formation is a fluvial sandstone containing uranium in both the Jackpile and St. Anthony mines.[27,28] The Jackpile mine is located on Native American land and was once the largest open-pit uranium mine in the world.[14] The Rio Paguate flows through the Jackpile mine. Previous studies found uranium concentrations of 772 μg L^{-1} U in filtered river water collected in the mine,[15] which is well above the 30 μg L^{-1} Environmental Protection Agency's (EPA) maximum contaminant level (MCL) for drinking water.[16] There are descriptions of the Jurassic-aged Jackpile member in the literature,[17−19] but the fate and transport of uranium daughter products are not well studied or fully understood.[15,20−24] Two studies conducted in the 1980s provided radium concentrations in surface and groundwater in the vicinity of the Jackpile mine and the downstream Mesita Dam reservoir (Figure 1).[25,26]

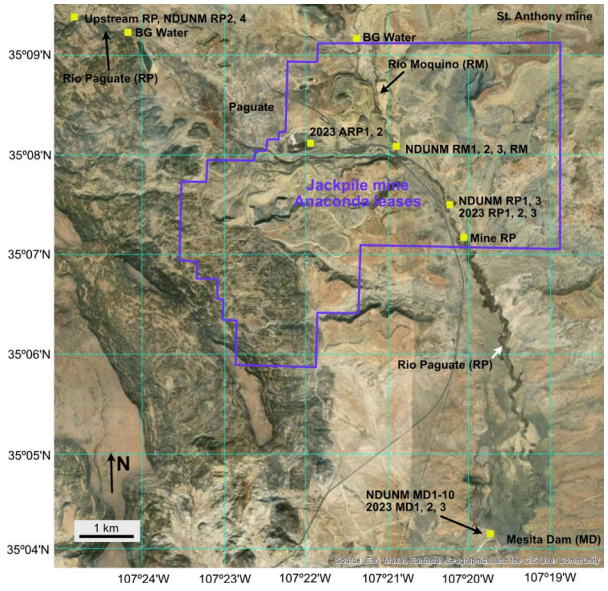

Figure 1. Map showing sample locations surrounding Pueblo of Laguna, New Mexico.

The Jackpile member is a sandstone formation that is composed primarily of quartz, potassium feldspar, and plagioclase, with clay, calcite, and organic matter cementing the sandstone.[27,28] It contains petrified wood, irregularly distributed plant remains, and "coal-like" material with portions containing 30−40% organic humate.[27] Up to 44% organic matter by volume occurs in sandstone from the Jackpile mine.[22] High concentrations of metals occur in zones within the Jackpile sandstone that are rich in humic organic material.[22,27] The Jackpile ore contains uranium mostly as unidentified U-organic complexes and coffinite, U-$(SiO_4)_{1-x}(OH)_{4x}$.[28,27,24]

The current study focuses on quantifying the activity ratio (^{226}Ra/^{238}U) of parent (^{238}U) and daughter (^{226}Ra) products in sediments and water collected in the Jackpile and St. Anthony mines, as well as water and sediment samples collected upstream and downstream from the Jackpile mine along Rio Paguate, Rio Moquino, and from the reservoir of the Mesita Dam (Figure 1). An earlier study investigated uranium concentrations in water and sediment samples collected along the Rio Paguate and Rio Moquino upstream, within, and downstream of the Jackpile mine, as well as in the wetland area of the Paguate reservoir above the Mesita Dam.[15]

MATERIALS AND METHODS

Field Sampling. Samples of water and sediment were collected during September 2021, and in May and August 2023, along Rio Paguate (RP), Rio Moquino (RM), and from the Mesita Dam (MD) reservoir that stores water in a wetland often referred to locally as Paguate Reservoir. The Mesita Dam was built about three decades prior to commencement of mining operations. Sediment and water samples were collected from Rio Paguate upstream from the Jackpile mine to establish radionuclide levels unimpacted by the Jackpile mine. Sediment samples from the Jackpile and St. Anthony mines were collected in 2017. A pond in the Jackpile mine North Pit ("North Pit Pond") and adjacent to the Rio Paguate (ARP) was sampled only in 2023. Sediment samples were collected from depths not exceeding 15 cm, and sediments collected from rivers were from the corresponding riverbed and not the floodplain. The sample collection sites are plotted in Figure 1 and coordinates are given in Tables 1 and 2. Note that the mine samples were collected from hotspots identified using a Geiger counter and are not representative of the average bulk material at the site.

At Rio Paguate, Rio Moquino, and the Mesita Dam reservoir, water collection bottles were rinsed using local water before collection. To minimize the possibility of cross contamination, nitrile gloves were worn during each collection event. Sample bottles were labeled with the date, time, sample number, and location. Samples were collected in duplicate and/or triplicate. After collection, samples were sealed and transported to the laboratory.

Water and sediment samples collected in May and August 2023, each weighing ∼1 kg, were sent to Energy Northwest in Richland, Washington, for radionuclide quantification with an HPGe detector. The objective was to establish ^{226}Ra levels from areas around the mine that had previously been demonstrated to have relatively low uranium concentrations.[15] These areas included Rio Paguate surface water and water in the reservoir of the Mesita Dam (refer to Tables S12−S14).

Water samples were analyzed without filtration to obtain a bulk assessment of radionuclide content. The water samples were colorless and clear but likely contained some sediments. Gamma counting for two samples collected from the North Pit Pond (ARP) indicated high activities of ^{226}Ra and other U-decay-scheme radionuclides (see below, Table 2). Subsequently, these water samples were passed through a 0.2 μM filter prior to further analysis by gamma spectroscopy at Energy Northwest (Table 2).

Elemental Analyses. Concentrations of U were measured using inductively coupled plasma-optical emission spectroscopy (ICP-OES) or ICP-mass spectrometry (MS). Solutions from the sequential extractions (see below) were digested in a class 1000 clean room facility at the Midwest Isotope and Trace Element Research Analytical Center (MITERAC), University of Notre Dame, and were analyzed using an Attom (Nu Instruments) high-resolution (HR)-ICP-MS instrument. The instrument was tuned and calibrated using a multielement solution. Measurements were also carried out at the University of New Mexico (UNM) using a PerkinElmer Optima 5300DV ICP-OES with a detection limit of 0.5 mg

https://doi.org/10.1021/acs.est.4c01257
Environ. Sci. Technol. 2024, 58, 15138−15146

Table 1. Analysis of ^{226}Ra and ^{238}U of Sediment and Rock Samples by γ-Spectroscopy[a]

	Lat.	Long.	$^{226}Ra/^{238}U$	^{226}Ra (pCi g^{-1})	MDA ^{226}Ra (pCi g^{-1})	^{238}U (pCi g^{-1})
St. Anthony Mine NDUNM 1.0	35.163	−107.304	16 ± 2.9	1727 ± 32	17	111 ± 20
St. Anthony Mine NDUNM 1.2			6.4 ± 1.3	1770 ± 53	39	277 ± 53
St. Anthony Mine NDUNM 2.0	35.163	−107.304	0.87 ± 0.20	857 ± 111	15	985 ± 180
St. Anthony Mine NDUNM 2.2			1.1 ± 0.23	1141 ± 125	19	1088 ± 204
St. Anthony Mine NDUNM 3.1	35.166	−107.317	3.2 ± 0.69	592 ± 34	33	184 ± 38
St. Anthony Mine NDUNM 3.2			4.8 ± 1.2	778 ± 43	11	163 ± 39
St. Anthony Mine NDUNM 4	35.166	−107.317	0.76 ± 0.21	603 ± 115	13	795 ± 162
Jackpile Mine NDUNM 5			1.1 ± 0.26	353 ± 46	40	324 ± 63
Jackpile Mine NDUNM 6				<39	39	89 ± 4.4
Jackpile Mine NDUNM 7	35.127	−107.340	0.34 ± 0.13	381 ± 127	37	1133 ± 210
River Sample NDUNM RP1	35.124	−107.340		<27	27	18 ± 8.3
River Sample NDUNM RP2	35.157	−107.414		<31	31	
River Sample NDUNM RP3	35.124	−107.340		<30	30	6.3 ± 1.5
River Sample NDUNM RP4	35.157	−107.414		<27	27	
River Sample NDUNM RM1	35.135	−107.347		<26	26	
River Sample NDUNM RM2	35.135	−107.347		<28	28	
River Sample NDUNM RM3	35.135	−107.349		<28	28	
Reservoir NDUNM MD1	35.069	−107.327		<21	21	15 ± 2.8
Reservoir NDUNM MD2	35.069	−107.327		<22	22	15 ± 2.8
Reservoir NDUNM MD3	35.069	−107.328		<23	23	<30
Reservoir NDUNM MD4	35.157	−107.414		<19	19	21 ± 4.1
Reservoir NDUNM MD5	35.069	−107.327		<22	22	<28
Reservoir NDUNM MD6	35.067	−107.326		<20	20	52 ± 10
Reservoir NDUNM MD7	35.069	−107.327		<24	24	<31
Reservoir NDUNM MD8	35.069	−107.327		<19	19	6.5 ± 1.8
Reservoir NDUNM MD9	35.069	−107.327		<25	25	64 ± 12
Reservoir NDUNM MD10	35.069	−107.327		<24	24	16 ± 5.6

[a]Samples NDUNM 1−3 were analyzed in duplicate.

Table 2. Analysis of Surface Water Samples Collected from Pueblo of Laguna[a]

Sample	Lat.	Long.	^{226}Ra pCi L^{-1}	^{238}U pCi L^{-1}	^{234}Th pCi L^{-1}	^{214}Pb pCi L^{-1}	^{214}Bi pCi L^{-1}	U (μg L^{-1})
Water samples collected in September 2021								
Upstream RP 1	35.157	−107.414						12 ± 0.6
Upstream RP 2	35.157	−107.414						15 ± 1.6
Mine RP 1	35.120	−107.340						250 ± 37
Mine RP 2	35.120	−107.340						216 ± 30
Mine RP 3	35.120	−107.340						218 ± 37
RM 1	35.135	−107.347						85 ± 7.5
RM 2	35.135	−107.347						82 ± 1
RM 3	35.135	−107.347						85 ± 1
MD	35.061	−107.330						13 ± 1.4
Water samples collected in May and August 2023								
2023 RP 1	35.125	−107.337	195 (82)	n.d.	8.3 (3.87)	16.8 (8.09)	16.0 (5.88)	
2023 RP 2	35.124	−107.337	191 (121)	n.d.	n.d.	27.6 (10.8)	14.2 (14)	
2023 RP 3	35.125	−107.337	229 (113)	n.d.	304 (184)	n.d.	n.d.	
2023 ARP 1	35.135	−107.365	1240 (154)	1330 (46)	1020 (279)	19.6 (10.8)	17.8 (11.4)	3950[b]
2023 ARP 1 Filtered			1350 (118)	1610 (364)	1540 (206)	n.d.	n.d.	4830[b]
2023 ARP 2	35.135	−107.365	1430 (157)	1560 (419)	1000 (315)	27.3 (14)	41 (13.4)	4680[b]
2023 ARP 2 Filtered			1370 (94)	1400 (296)	1670 (178)	13.2 (6.74)	n.d.	4200[b]
2023 MD 1	35.066	−107.327	249 (111)	n.d.	445 (227)	n.d.	n.d.	
2023 MD 2	35.066	−107.326	211 (107)	n.d.	n.d.	16.2 (9.3)	n.d.	
2023 MD 3	35.070	−107.329	227 (118)	n.d.	11 (4.25)	n.d.	n.d.	

[a]The activities are from gamma spectroscopy and U concentrations are by ICP-MS. Samples were from Rio Paguate (RP), Rio Moquino (RM), a pond of standing water in the Jackpile mine North Pit that is adjacent to the Rio Paguate (ARP), and the Mesita Dam reservoir (MD). Most samples were analyzed without filtration. ARP 1 and ARP 2 were also filtered through a 2 μm filter prior to analysis. For gamma spectroscopy measurements, the minimum detectable activity (MDA) is given in parentheses. For samples collected in May and August, 2023, radionuclides that were not detected are so noted (n.d.). [b]converted from pCi L^{-1}.

L^{-1}. When lower detection limits were required, measurements at UNM were done with a PerkinElmer NexION 300D (Dynamic Reaction Cell) ICP-MS with a detection limit of 0.5 μg L^{-1}. Both instruments at UNM were calibrated with Fischer

https://doi.org/10.1021/acs.est.4c01257
Environ. Sci. Technol. 2024, 58, 15138−15146

Scientific standards with a five-point calibration curve, and quality assurance and quality control (QA/QC) measures were taken. All measurements were conducted in triplicate and the error stated is the standard deviation.

Gamma Spectroscopy. Approximately 2 g of dry sediment samples were used for gamma counting at the University of Notre Dame. Freeze-drying was performed to remove moisture from damp samples. The samples were then placed in 5 × 7.6 cm polyethylene bags, triply contained to avoid dispersion of sediments. The samples were molded to less than 2 cm thick and 5 × 5 cm for γ-spectroscopy analysis to allow the sample to be close in size to the calibration point sources.

Following packaging, samples were transferred to a lead-shielded counting station consisting of a 10 cm-thick lead castle equipped with an HPGe detector. A Canberra standard electrode coaxial germanium detector was used (model # GC3518). The detector was attached to a 30-L ultralow background cryostat, which was filled continuously with liquid N_2 throughout the counting duration.

The detector was calibrated for energy and efficiency using a set of standard calibration sources from Amersham International Limited (^{60}Co, ^{133}Ba, ^{137}Cs, and ^{241}Am) and Isotope Products Laboratories (^{152}Eu). The channel number was converted to energy to ensure accurate peak assignments (Figure S1). ^{137}Cs was used for monitoring efficiency changes; minor effects in energy drift were observed (Figure S2). Decay radiation information such as the intensity of the γ-rays (I_γ) was obtained from the National Nuclear Data Center (NNDC).[29−36] Efficiency and corresponding energies were plotted using OriginPro and fitted according to a user-defined function described in the literature for HPGe detectors (Figure S3 a−c).[37]

Activity measurements were performed with Ortec's Maestro data acquisition software. Peaks were fitted with Maestro-Pro (Version 9) using a 5-background point average at the region of interest and errors were propagated. Blanks were collected to determine the background rate for peaks of interest (peak counts/time) for background subtraction.

The method of De Corte et al. was followed for ^{226}Ra quantification that treats the system as if ^{238}U and its immediate daughter isotope ^{234}Th ($t_{1/2}$ = 24 days) are in equilibrium and that ^{235}U and ^{238}U are at natural isotopic abundance as shown by eq 1.[38] The method involves obtaining the net peak area at the 63 keV line attributable to ^{234}Th (63.29 keV I_γ = 3.7%) and accounting for the interference from ^{232}Th (63.81 keV I_γ = 0.263%) by utilizing the 338 keV line of ^{228}Ac (338.32 keV I_γ = 11.27%). We also used the ^{234}Th line at 63 keV to quantify ^{238}U as it cannot be directly determined from its weakly emitted photons.[39] The contribution of ^{235}U was determined and subtracted to obtain total ^{226}Ra counts at 186 keV because the ^{235}U line (I_γ= 57.0% 185.71 keV) at 186 keV overlaps with the most intense spectral line of ^{226}Ra (I_γ= 3.64% 186.21 keV). The activity of an isotope was determined with eq 2. Equation 1 is used to determine the ^{235}U contribution to the 186 keV line is

$$C[^{235}U_{185.7keV}] = C[^{234}Th_{63.3keV}] \frac{(I_\gamma \cdot \varepsilon \cdot TCS)_{185.7keV}}{(I_\gamma \cdot \varepsilon \cdot TCS)_{63.3keV}} \frac{(\theta \cdot \lambda)_{^{235}U}}{(\theta \cdot \lambda)_{^{238}U}} \quad (1)$$

Where C = total counts of the peak; I_γ = intensity of the peak; ε = efficiency of the detector; TCS = true coincidence summing;[40] θ = natural isotopic ratio (^{235}U: 0.720, ^{238}U: 99.2745); λ = decay constant s^{-1} (^{235}U: 3.121 × 10^{-17}, ^{238}U: 4.916 × 10^{-18}).

Equation 2 shows the activity of an isotope is determined by using the following equation:

$$A = \frac{R}{\varepsilon \cdot I_\gamma} = \frac{C}{\varepsilon \cdot I_\gamma \cdot t} \quad (2)$$

Where A = activity of an isotope; R = detected gamma rate; ε = efficiency of the detector; I_γ = intensity of the peak; C = total counts of the peak; t = duration of the measurement

Gamma spectroscopy done by the Energy Northwest laboratory was done using Ortec HPGe detectors and followed similar procedures as the measurements done at the University of Notre Dame. At Energy Northwest, the detectors were calibrated for energy and efficiency using a set of standard calibration sources from Ekert and Zigler (^{109}Cd, ^{57}Co, ^{60}Co, ^{139}Ce, ^{203}Hg, ^{113}Sn, ^{88}Y, ^{137}Cs, ^{241}Am). The channel number was converted to energy to ensure accurate peak assignments. ^{109}Cd, ^{57}Co, ^{60}Co, ^{139}Ce, ^{137}Cs, and ^{241}Am were used for monitoring efficiency changes daily; only minor effects of drift are rarely observed and are adjusted for during daily quality control (QC) procedures. Activity measurements were done with Ortec's Gamma Vision 32 data acquisition software and libraries. The instruments were checked daily for background and quarterly for long backgrounds. Prior to running a calibrated geometry, the instruments were checked with the same geometry against known values for standards. All detectors were calibrated with newly purchased sources each year.

The minimum detectable activity (MDA) for radionuclides in each sample is defined as the least amount of activity that can be confidently measured by gamma spectrometry.[40] In the current work, corresponding MDAs for radionuclides in each sample were estimated using the method provided in Gilmore.[40]

Sequential Extractions. Sequential extraction of U was performed on sediments from sampling sites NDUNM 1 and 2 because these exhibited distinct ^{226}Ra/^{238}U activity ratios, with NDUNM 1 in disequilibrium and NDUNM 2 near secular equilibrium (Table 1). Details pertaining to the sequential extraction experiments are available in the Supporting Information.

Additional Analyses. Selected samples were analyzed for mineralogy using powder X-ray diffraction (pXRD). Element maps for sediment samples were created using X-ray fluorescence (XRF) and images were collected using a scanning electron microscope (SEM). Organic carbon was quantified, and gas chromatography−mass spectrometry was done for selected sediment samples. The details of each of these methodologies and the instruments used are in the Supporting Information

RESULTS AND DISCUSSION

A thorough examination of U-series geochemistry is provided by Bourdon et al.,[41] who provide essential background covering basic topics in radiochemistry including half-life and activity, secular equilibrium, and causes of disequilibrium in the U-series. Two mechanisms that can disrupt secular equilibrium in the U-series are fractionation due to the different chemical behaviors of the radionuclides (including various geochemical reactions), and radioactive decay wherein

https://doi.org/10.1021/acs.est.4c01257
Environ. Sci. Technol. 2024, 58, 15138−15146

recoil effects can be important, especially in low-temperature environments.[41] Such effects can result in ejection of a daughter radionuclide from a solid if the decay event occurred sufficiently close to the edge of the particle, and accumulation of radiation damage in a mineral can increase its susceptibility to various forms of alteration.

Note that when comparing the activities for water and sediments in Tables 1 and 2 and the subsequent discussion, it is important to note that these are reported per liter and gram, respectively.

Quantification of Radium and Uranium in Materials from Mines. Samples from the Jackpile and St. Anthony mines within the Jackpile member exhibited the highest concentrations of ^{238}U and ^{226}Ra among all the samples analyzed. The mine samples, specifically NDUNM 1−7, were taken from areas of high activity selected using a Geiger counter and likely correspond to variously weathered uranium ore.

NDUNM 1, analyzed in duplicate, yielded activity ratios ($^{226}Ra/^{238}U$) at 16 ± 2.9 and 6.4 ± 1.3, indicating preferential removal of uranium likely by weathering (Table 1). The measured activity ratios of NDUNM 2 are 0.87 ± 0.20 and 1.1 ± 0.23, indicative of pristine uranium ore near secular equilibrium. The measured activity ratios for NDUNM 3 of 3.2 ± 0.69 and 4.8 ± 1.2 indicate preferential uranium removal, although not as extensively as for NDUNM 1. Samples NDUNM 4 and 5 yielded activity ratios consistent with secular equilibrium and pristine ore, ^{226}Ra was below the detection limit for NDUNM-6, and NDUNM-7 is in disequilibrium and potentially corresponds to accumulation of uranium (see below).

Activity ratios ($^{226}Ra/^{238}U$) of 0.5 to 9 have been observed in organic-rich sediments collected in Ireland,[7] whereas ratios greater than and less than one have been observed in roll-front uranium deposits.[9] The uranium in the Jackpile member is a roll front deposit and contains high total organic carbon.[22] Deviations from an activity ratio of one (5.9−165.8)[10] have been observed in the vascular system of plants (Russia) and in water samples from hot spring deposits (1.79−2115) (Morocco).[42] In a 1961 study, researchers sampled ore from the upper Jackpile member in northwestern New Mexico and found that the activity of several daughter products was in excess in low-grade ore and deficient in high-grade ore.[43] Geologic processes cause the departure of activity ratios from secular equilibrium. Our analyses show that deviations from secular equilibrium can occur, as for samples NDUNM 1, 3, and 6.

The pXRD results for NDUNM 1−3 from the St. Anthony Mine revealed only quartz (Figure S5a), consistent with sandstone. The detection limit for pXRD is on the order of a few weight percent. XRF analysis indicated the presence of uranium and various elements (Figures S6−S11, Tables S4−S5). The PXRD of NDUNM 4 also indicated mostly quartz; however, the sample also contained a substantial quantity of the uranyl phosphate autunite (Figure S5a).

XRF analysis of various locations on NDUNM 3 from the St. Anthony Mine revealed barely detectable uranium and high levels of Mg and Ca (Figure S10 and Table S6 for XRF elemental analysis). This observation aligns with the higher measured activity of ^{226}Ra in comparison to ^{238}U, a consistency attributed to the geochemical properties of Ra, which are similar to other divalent cations.

The XRF map and spot analyses of NDUNM 4 from the St. Anthony Mine indicated substantial U and P, as well as Fe, V, and S (Figure S12−S14 and Table S7). In their oxyanion forms, vanadyl and sulfate can both coordinate the uranyl ion, and Fe oxides or oxyhydroxides can act as adsorbent minerals for U-bearing species. NDUNM 4 contained a $^{226}Ra/^{238}U$ ratio of 0.76 ± 0.21, which is at secular equilibrium within uncertainty. We hypothesize this is a result of uranium retention as the relatively insoluble uranyl phosphate mineral, autunite (Figure S5a).

Samples NDUNM 5 and 6 from the Jackpile Mine contained ^{238}U activities of 324 ± 63 and 89 ± 4.4 pCi g^{-1}, respectively, with ^{226}Ra concentrations below the MDA for NDUNM 6. For riverbank sediments, NDUNM RP 1 and RP 3, collected from Rio Paguate where the river intersects the Jackpile mine, activities of 18 ± 8.3 and 6.3 ± 1.5 pCi g^{-1} of ^{238}U were detected, with ^{226}Ra below the MDA. The XRF analyses of these samples indicated various elements, including S, Al, Ti, and Fe (Figures S15−S18, Tables S8−S10). pXRD results for NDUNM RP 1 and RP 3 indicated the prevalence of quartz and calcite (Figure S5b). These samples are similar in that they all contain relatively low uranium concentrations, and the characterization of uranium association using the employed techniques did not lead to conclusive interpretations. This reflects the challenges of obtaining meaningful data in situations involving extremely low uranium concentrations and underscores the difficulties associated with determining phases controlling uranium water concentrations, as highlighted by previous researchers.[1]

Quantification of Radium and Uranium in Sediments and Water in Rio Paguate Upstream from the Mine. The activities of ^{226}Ra and ^{238}U in sediments collected from the stream bed of the Rio Paguate upstream from the mine were below the MDA of the gamma counting method at UND. Water samples collected at the same location had concentrations of 12−15 $\mu g\ L^{-1}$ U as determined by ICP-MS (Table 2). A study conducted several years ago found only low U concentrations in water collected upstream from the mine at a similar location, with a maximum concentration of 8 $\mu g\ L^{-1}$ observed.[15]

Quantification of Radium and Uranium in Sediments and Water from Rio Paguate Impacted by the Mine. Surface water samples collected from Rio Paguate in 2021 where the river flows through what had been the Jackpile mine contained uranium concentrations of approximately 225 $\mu g\ L^{-1}$ U (0.084 pCi g^{-1}) at the time of sampling (Table 2). Radium was not quantified in these samples because their volumes were too low (larger samples were taken in 2023). Previous studies conducted in a similar sampling location of Rio Paguate have reported uranium concentrations in the 500−700 $\mu g\ L^{-1}$ range.[15,22,23]

Water samples collected from Rio Paguate inside the Jackpile mine in 2023 (Figure 1) contained ^{226}Ra activities of 205 ± 21 pCi L^{-1} (Table 6 and Table S14). Radium activities in a pond that formed on top of backfill in the Jackpile mine North Pit ("North Pit Pond") and adjacent to the Rio Paguate (ARP) were several times higher. In these samples, ^{226}Ra activities in unfiltered water (ARP 1 and ARP 2) were 1330 and 1560 pCi L^{-1} and the $^{226}Ra/^{238}U$ ratios are close to one (Table 2 and Table S14). Recounting of samples ARP 1 and ARP 2 after they had been passed through a 0.2 μm filter yielded ^{226}Ra concentrations of 1610 and 1400 pCi L^{-1} with $^{226}Ra/^{238}U$ ratios close to one.

https://doi.org/10.1021/acs.est.4c01257
Environ. Sci. Technol. 2024, 58, 15138−15146

Table 3. ICP-MS Measurement of Total Uranium Leached (mg L^{-1})

	NDUNM 1.1	NDUNM 1.2	NDUNM 2.1	NDUNM 2.2
Water-soluble	2.75 ± 0.14	0.63 ± 0.03	1.44 ± 0.07	1.44 ± 0.07
Exchangeable	0.15 ± 0.01	0.17 ± 0.01	3.58 ± 0.18	4.47 ± 0.22
Oxidizable	0.47 ± 0.02	0.30 ± 0.02	0.31 ± 0.02	0.27 ± 0.01
Acid Soluble	24.26 ± 1.21	29.95 ± 1.50	236 ± 12	182.2 ± 9.1
Reducible	21.25 ± 1.06	27.56 ± 1.38	188.8 ± 9.4	215 ± 11
Residual	218 ± 11	208 ± 10	(8.24 ± 42)x10^3	(5.02 ± 25)x10^3

Water samples ARP 1 and 2 had sufficiently high activities for the quantification of ^{226}Ra, ^{234}Th, ^{214}Pb, and ^{214}Bi. The activities of ^{226}Ra and ^{234}Th are similar indicating that they are likely in secular equilibrium. Those of ^{214}Pb and ^{214}Bi are much lower, which indicates that ^{222}Rn has escaped from the samples. The half-lives of ^{218}Po, ^{214}Pb and ^{214}Bi are all less than 30 min, so their absence indicates loss of radon gas.

Note that a ^{226}Ra activity of 1000 pCi L^{-1} similar to ARP 1 and 2 corresponds to a concentration of 0.001 μg L^{-1}. Gamma counting is generally the only viable method for quantification of ^{226}Ra in environmental samples.

Quantification of Radium and Uranium in Sediments and Water from Rio Moquino. Investigation of the Rio Moquino section, situated adjacent to the Jackpile mine, revealed uranium water concentrations of approximately 82−85 μg L^{-1} by ICP-MS (0.029 pCi g^{-1}) (Table 2). The uranium levels in sediment samples were below the MDA using our γ-spectrometer setup and methods, with a measured concentration of 1.5 ± 0.28 (pCi g^{-1}) for ^{238}U in NDUNM RM 1 (Table 1).

The pXRD analyses of sediment samples from Rio Moquino revealed mostly calcite (Figure S5b). Similarly, NDUNM RM 1 and RM 3 consisted of calcite, with ^{226}Ra levels below the MDA.

Quantification of Radium and Uranium in Sediments and Water from Mesita Dam. Water samples collected from the Mesita Dam reservoir in Pueblo of Laguna located 5 miles south (downstream) of the Jackpile mine contained 13 ± 1.4 μg L^{-1} U. Sediment samples collected in the vicinity of the dam, including where water was seeping beneath the dam, contained no detectable levels of ^{226}Ra and ^{238}U values ranging from below the MDA to 64 ± 12 pCi g^{-1} (Table 1). The presence of uranium in the samples taken near the dam, in the absence of detectable radium, could indicate that the uranium was transported in aqueous solution rather than as sediment.

Samples NDUNM MD 1, MD 2, and MD 4 contained 15 ± 2.8, 15 ± 2.8, and 21 ± 4.1 pCi g^{-1} of ^{238}U, and were primarily composed of thenardite (Na_2SO_4). The white thenardite deposits are evident in aerial photos and pXRD (Figure S5c). Samples in which S was detected by XRF generally also contain detectable quantities of ^{238}U (Table S11).

Water collected from the Mesita Dam reservoir in 2023 contained an average ^{226}Ra concentration of 229 ± 19 pCi L^{-1} (Table 2), while surface sediments collected near the Mesita Dam contained 7 pCi g^{-1} (Table S13). A study in 1983 reported elevated ^{226}Ra in sediments from the Mesita Dam reservoir, with the highest value found for any radionuclide being ^{226}Ra at 26.85 pCi g^{-1} for sediments at a depth of 15−30 cm.[25]

The aqueous solubility of uranyl sulfates and radium sulfate differs dramatically. Uranyl sulfate minerals are relatively soluble,[44] and various studies have demonstrated that uraninite in mine wastes undergoes alteration together with oxidation of sulfide minerals, contributing to uranium dissolution through the formation of uranyl sulfate complexes.[45−47] In contrast, radium sulfate is the least soluble among alkali earth divalent cation sulfates and is environmentally insoluble.[48,49] Within the Jackpile member in Ambrosia Lake, previous researchers identified radium-rich Barite ($BaSO_4$) in close proximity to uranium ore.[43] Radium had migrated a short distance, with a substantial amount rarely identified outside the ore vicinity.[43]

Activities of ^{226}Ra may exhibit variability dependent on precipitation patterns, as observed previously at the Jackpile mine in the case of uranium concentrations ranging from 35 to 772 μg L^{-1} with the highest U concentrations observed during times of heavy rainfall.[15] Researchers suggested a complex interplay between hydrological factors and local geochemical conditions as explanations for the observed variability.[15] Radium activity seasonal variability is likely in many systems such as observed along coastlines attributed to groundwater discharge.[50,51]

Uranium Association in St. Anthony Mine Samples NDUNM 1 and 2. Sequential extractions provided insight into leachable fractions under specific conditions, but the method does not mimic the complexity of natural systems, including adsorption, desorption, solubility, and aqueous complexation.[52] The results of the sequential extraction experiments, based on duplicate analyses, indicated that almost 90% of the U in NDUNM 2 was in the residual fraction, compared to about 80% in NDUNM 1 (Table 3). Combining the reducible and acid-soluble fractions accounted for approximately 20% of the U in NDUNM 1 and about 5% in NDUNM 2. Despite representing less than 1% of the total U in both samples, the water-soluble fraction contained concentrations above 1 ppm, with approximately 1% of the total U in NDUNM 1 leaching out, while less than 0.02% does so for NDUNM 2. The substantial difference in U leaching, particularly in the water-soluble fraction between NDUNM 1 and 2, may contribute to the observed variations in $^{226}Ra/^{238}U$ ratios presented in Table 1.

NDUNM 1 and 2 contained carbon at 3.1% ± 1.8 and 7.8 ± 1.2 wt %, respectively. The presence of nitrogen was negligible in NDUNM 1 and 0.09% ± 0.03 wt % in NDUNM 2. The loss-on-ignition (LOI) method[53,54] and SEM imaging of NDUNM 1 and 2 samples revealed organic material (Figure S20). This is consistent with previous studies of Jackpile sandstone that found more than 50% organic material associated with quartz,[55] with organic matter acting as a cementing agent. GC-MS analysis of NDUNM 1 and 2 revealed a complex mixture of organic matter, including hydrocarbons and organic acids. Of particular interest is the presence of acetic acid in NDUNM 1 and not in NDUNM 2 (Figure S21), which can act as an anion in solution and increase the concentration of uranium through aqueous complexation.

https://doi.org/10.1021/acs.est.4c01257
Environ. Sci. Technol. 2024, 58, 15138−15146

Previous research identified various types of organic matter in the Jackpile member, including humic, fulvic, and low-grade coal.[22,27,43,56,57] While the organic matter present in the Jackpile member has been described as relatively insoluble,[43] its breakdown by oxidation and bacteria has been reported.[27] Both humic and fulvic acids can play a role in uranium transport in the Jackpile mine.[22] We hypothesize that the breakdown of organic matter linked to the presence of relatively small organic acids, such as acetic acid, also contributes to the transport of uranium at the site.

Overview of Radionuclide Distribution at Laguna Pueblo. Water samples collected from Rio Paguate upstream from the Jackpile mine during the current study and by previous researchers contain uranium concentrations that are below the EPA MCL of 30 $\mu g\ L^{-1}$. The presence of uranium in surface water in the region is expected given the geology of the area.

Radioactive sediments and rocks in the Jackpile and St. Anthony mines are the likely sources of radionuclides in surface water flowing through the mine. Analysis of ^{226}Ra and ^{238}U in several samples collected from hotspots identified using a Geiger counter showed that some are in secular equilibrium, indicating they are relatively pristine. Others have $^{226}Ra/^{238}U$ ratios well above one, which indicates preferential removal of uranium, most likely by weathering and transport of uranium away in water. Some samples have $^{226}Ra/^{238}U$ ratios well under one, which indicates relatively recent accumulation of uranium, perhaps as insoluble phosphate minerals.

Whereas Rio Paguate samples unimpacted by the mine contained no more than 15 $\mu g\ L^{-1}$ of uranium on the day of sampling, water collected from the same river within the mine boundaries contained 216−250 $\mu g\ L^{-1}$ uranium (Table 2). Water flowing in the mine in Rio Moquino also contained elevated uranium concentrations at 82−85 $\mu g\ L^{-1}$. Water collected in Rio Paguate within the mine boundaries contained 195−229 pCi L^{-1} ^{226}Ra.

Sediment and water samples taken in the vicinity of the Mesita Dam (Figure 1) are likely impacted by the release of radionuclides from water upstream in the mine. Water collected from the reservoir upstream from Mesita Dam contained 211−249 pCi L^{-1} ^{226}Ra, which is indistinguishable from the activity measured for river water collected within the mine boundaries. Sediments collected around Mesita Dam contained less ^{226}Ra.

The highest activities of ^{226}Ra and ^{238}U in water samples collected during the current study were in water obtained from the North Pit (ARP 1 and 2), which is a standing body of water within the mine. In these samples, ^{238}U, ^{234}Th and ^{226}Ra are in equilibrium, but radon gas has escaped at some point prior to analysis. The current EPA standards for alpha emitters in safe drinking water combine ^{226}Ra and ^{228}Ra, setting the limit at 5 pCi L^{-1}. There is also a gross alpha standard for all alphas of 15 pCi L^{-1}, not including radon and uranium. All water samples collected within the mine and downstream from the mine contained vastly more alpha emitters than the EPA standard. Notably, livestock were inside the fence around the North Pit on the day of sampling in 2023, which can serve as a vector for radionuclide transport and requires further study.

■ ASSOCIATED CONTENT

Supporting Information

The Supporting Information is available free of charge at https://pubs.acs.org/doi/10.1021/acs.est.4c01257.

Details for analytical techniques: gamma spectroscopy, powder X-ray diffraction, X-ray fluorescence, scanning electron microscopy, elemental analyses, sequential extractions, organic carbon quantification, and gas chromatography−mass spectrometry (PDF)

■ AUTHOR INFORMATION

Corresponding Author

Peter C. Burns − *Department of Civil and Environmental Engineering and Earth Sciences, University of Notre Dame, Notre Dame, Indiana 46556, United States; Department of Chemistry and Biochemistry, University of Notre Dame, Notre Dame, Indiana 46556, United States;* orcid.org/0000-0002-2319-9628; Email: pburns@nd.edu

Authors

Virginia G. Rodriguez − *Department of Civil and Environmental Engineering and Earth Sciences, University of Notre Dame, Notre Dame, Indiana 46556, United States;* orcid.org/0000-0002-8728-4004

Ashabari Majumdar − *Department of Physics and Astronomy, University of Notre Dame, Notre Dame, Indiana 46556, United States*

Isabel Meza − *Department of Civil, Construction & Environmental Engineering, MSC01 1070, University of New Mexico, Albuquerque, New Mexico 87131, United States; Center for Water and the Environment, University of New Mexico, Albuquerque, New Mexico 87131, United States*

Loretta Corcoran − *Department of Civil and Environmental Engineering and Earth Sciences, University of Notre Dame, Notre Dame, Indiana 46556, United States*

Amanda Pierson − *Energy Northwest, Richland, Washington 99354, United States*

Kaelin Gagnon − *Department of Civil, Construction & Environmental Engineering, MSC01 1070, University of New Mexico, Albuquerque, New Mexico 87131, United States*

Caitlyn Cano − *Department of Civil and Environmental Engineering and Earth Sciences, University of Notre Dame, Notre Dame, Indiana 46556, United States*

Abdul-Mehdi S. Ali − *Department of Earth and Planetary Sciences, MSC03 2040, University of New Mexico, Albuquerque, New Mexico 87131, United States*

Christopher M. Shuey − *Southwest Research and Information Center, Albuquerque, New Mexico 87106, United States*

Gregory Jojola − *Pueblo of Laguna Environment and Natural Resources Department, Pueblo of Laguna, New Mexico 87038, United States*

Wanpeng Tan − *Department of Physics and Astronomy, University of Notre Dame, Notre Dame, Indiana 46556, United States*

Ani Aprahamian − *Department of Physics and Astronomy, University of Notre Dame, Notre Dame, Indiana 46556, United States*

José M. Cerrato − *Department of Civil, Construction & Environmental Engineering, MSC01 1070, University of New Mexico, Albuquerque, New Mexico 87131, United States;* orcid.org/0000-0002-2473-6376

Complete contact information is available at: https://pubs.acs.org/10.1021/acs.est.4c01257

Notes

The authors declare no competing financial interest.

https://doi.org/10.1021/acs.est.4c01257
Environ. Sci. Technol. 2024, 58, 15138−15146

■ ACKNOWLEDGMENTS

We thank the Environmental and Natural Resources Department (ENRD) at the Pueblo of Laguna for access to Laguna Lands and Kyle Swimmer for fieldwork. V.G.R. was supported by a National Science Foundation Graduate Research Fellowship (DGE-1841556) and the University of Notre Dame (UND) GLOBES interdisciplinary graduate training program. We thank the Nuclear Science Laboratory (NSL) at UND for access to gamma counting facilities (National Science Foundation PHY-2011890). The Center for Environmental Science and Technology (CEST) at UND provided access to the EDAX Orbis XRF and Costech ECS 4010 elemental analyzer. We thank the Materials Characterization Facility (MCF) for the use of the Bruker D8 Discovery and Bruker D8 Davinci diffractometers and the GC-MS. The MCF is funded by the Sustainable Energy Initiative (SEI), which is part of the Center for Sustainable Energy at Notre Dame (ND Energy). Researchers from the University of New Mexico (UNM) were supported by the National Science Foundation (CREST Award 1914490) and the National Institute of Environmental Health Sciences (Superfund Research Program Award 1 P42 ES025589), and the UNM Comprehensive Cancer Center. Any opinions, findings, conclusions, or recommendations expressed in this material are those of the author(s) and do not necessarily reflect the views of the National Science Foundation.

■ REFERENCES

(1) Maher, K.; Bargar, J. R.; Brown, G. E. Environmental Speciation of Actinides. *Inorg. Chem.* **2013**, *52*, 3510−3532.

(2) Romanchuk, A. Yu.; Vlasova, I. E.; Kalmykov, S. N. Speciation of Uranium and Plutonium From Nuclear Legacy Sites to the Environment: A Mini Review. *Front. Chem.* **2020**, *8*, 630.

(3) Dinis, M. de L.; Fiúza, A. Mitigation of Uranium Mining Impacts—A Review on Groundwater Remediation Technologies. *Geosci. J.* **2021**, *11*, 250.

(4) Prince, J. R. Comments on Equilibrium, Transient Equilibrium, and Equilibrium in Serial Radioactive Decay. *J. Nucl. Med.* **1979**, 162−164.

(5) *Uranium-Series Disequilibrium: Applications to Earth, Marine, and Environmental Sciences*, 2nd ed.; Ivanovich, M.; Harmon, R. S., Eds.; Clarendon Press: Oxford, U.K., 1992.

(6) Olley, J. M.; Murray, A.; Roberts, R. G. The Effects of Disequilibria in the Uranium and Thorium Decay Chains on Burial Dose Rates in Fluvial Sediments. *Quat. Sci. Rev.* **1996**, *15*, 751−760.

(7) Dowdall, M.; O'Dea, J. $^{226}Ra/^{238}U$ Disequilibrium in an Upland Organic Soil Exhibiting Elevated Natural Radioactivity. *J. Environ. Radioact.* **2002**, *59*, 91−104.

(8) Yunoki, E.; Kataoka, T.; Michihiro, K.; Sugiyama, H.; Shimizu, M.; Mori, T. Activity Concentration of ^{226}Ra and ^{238}U in Various Soils. *J. Radioanal. Nucl. Chem., Letters* **1992**, *166*, 331−341.

(9) Grozeva, N. G.; Radwan, J.; Beaucaire, C.; Descostes, M. Reactive Transport Modeling of U and Ra Mobility in Roll-Front Uranium Deposits: Parameters Influencing $^{226}Ra/^{238}U$ Disequilibria. *J. Geochem. Explor.* **2022**, *236*, 106961.

(10) Chevychelov, A.; Sobakin, P.; Gorokhov, A.; Kuznetsova, L.; Alekseev, A. Migration of ^{238}U and ^{226}Ra Radionuclides in Technogenic Permafrost Taiga Landscapes of Southern Yakutia, Russia. *Water* **2021**, *13*, 966.

(11) Molinari, J.; Snodgrass, W. J. The Chemistry and Radiochemistry of Radium and the Other Elements of the Uranium and Thorium Natural Decay Series; *International Atomic Energy Agency*: Vienna, 1990; Vol. *1*, pp 59−128.

(12) Navrotsky, A.; Shvareva, T.; Guo, X. *Uranium—Cradle to Grave*; Burns, P.; Sigmon, G., Eds.; Mineralogical Association of Canada: Winnipeg, Manitoba, Canada, 2013; Vol. *43*.

(13) McDevitt, B.; McLaughlin, M.; Cravotta, C. A.; Ajemigbitse, M. A.; Van Sice, K. J.; Blotevogel, J.; Borch, T.; Warner, N. R. Emerging Investigator Series: Radium Accumulation in Carbonate River Sediments at Oil and Gas Produced Water Discharges: Implications for Beneficial Use as Disposal Management. *Environ. Sci.: Processes Impacts* **2019**, *21*, 324−338.

(14) Moore-Nall, A. The Legacy of Uranium Development on or Near Indian Reservations and Health Implications Rekindling Public Awareness. *Geosci. J.* **2015**, *5*, 15−29.

(15) Blake, J. M.; De Vore, C. L.; Avasarala, S.; Ali, A.-M.; Roldan, C.; Bowers, F.; Spilde, M. N.; Artyushkova, K.; Kirk, M. F.; Peterson, E.; Rodriguez-Freire, L.; Cerrato, J. M. Uranium Mobility and Accumulation along the Rio Paguate, Jackpile Mine in Laguna Pueblo, NM. *Environ. Sci.: Processes Impacts* **2017**, *19*, 605−621.

(16) *National Primary Drinking Water Regulations*; EPA 816-F-09-004 ; Environmental Protection Agency, 2009 (accessed 2022-12-15).

(17) Turner, C. E.; Peterson, F. Reconstruction of the Upper Jurassic Morrison Formation Extinct Ecosystem—a Synthesis. *Sediment. Geol.* **2004**, *167*, 309−355.

(18) Owen, D. E.; Walters, L. J., Jr; Beck, R. G. The Jackpile Sandstone Member of the Morrison Formation in West-Central New Mexico-a Formal Definition. *New Mexico Geology* **1984**, *6*, 45−52.

(19) Foster, J. R. Aspects of Vertebrate Paleoecology, Taphonomy, and Biostratigraphy of the Morrison Formation (Upper Jurassic), Rocky Mountain Region, Western United States. *PhD*, University of Colorado at Boulder, Ann Arbor, 1998.

(20) Rodriguez-Freire, L.; DeVore, C. L.; El Hayek, E.; Berti, D.; Ali, A.-M. S.; Lezama Pacheco, J. S.; Blake, J. M.; Spilde, M. N.; Brearley, A. J.; Artyushkova, K.; Cerrato, J. M. Emerging Investigator Series: Entrapment of Uranium-Phosphorus Nanocrystals inside Root Cells of Tamarix Plants from a Mine Waste Site. *Environ. Sci.: Processes Impacts* **2021**, *23*, 73−85.

(21) El Hayek, E.; Torres, C.; Rodriguez-Freire, L.; Blake, J. M.; De Vore, C. L.; Brearley, A. J.; Spilde, M. N.; Cabaniss, S.; Ali, A.-M. S.; Cerrato, J. M. Effect of Calcium on the Bioavailability of Dissolved Uranium(VI) in Plant Roots under Circumneutral pH. *Environ. Sci. Technol.* **2018**, *52*, 13089−13098.

(22) Velasco, C. A.; Artyushkova, K.; Ali, A.-M. S.; Osburn, C. L.; Gonzalez-Estrella, J.; Lezama-Pacheco, J. S.; Cabaniss, S. E.; Cerrato, J. M. Organic Functional Group Chemistry in Mineralized Deposits Containing U(IV) and U(VI) from the Jackpile Mine in New Mexico. *Environ. Sci. Technol.* **2019**, *53*, 5758−5767.

(23) Avasarala, S.; Torres, C.; Ali, A.-M. S.; Thomson, B. M.; Spilde, M. N.; Peterson, E. J.; Artyushkova, K.; Dobrica, E.; Lezama-Pacheco, J. S.; Cerrato, J. M. Effect of Bicarbonate and Oxidizing Conditions on U(IV) and U(VI) Reactivity in Mineralized Deposits of New Mexico. *Chem. Geol.* **2019**, *524*, 345−355.

(24) Deditius, A. P.; Utsunomiya, S.; Ewing, R. C. The Chemical Stability of Coffinite, $USiO_4{\cdot}nH_2O$; $0 < n < 2$, Associated with Organic Matter: A Case Study from Grants Uranium Region, New Mexico, USA. *Chem. Geol.* **2008**, *251*, 33−49.

(25) Popp, C. J.; Hawley, J. W.; Love, D. W. *Radionuclide and Heavy Metal Distribution in Recent Sediments of Major Streams in the Grants Mineral Belt, New Mexico*; New Mexico Bureau of Geology and Mineral Resources, 1983.

(26) Momeni, M.; Tsai, S.; Yang, J.; Gureghian, A.; Dungey, C. *Radiological Impacts of Jackpile-Paguate Uranium Mines: An Analysis of Alternatives of Decommissioning*; Argonne National Laboratory, 1983.

(27) Adams, S.; Saucier, A. *Geology and Recognition Criteria for Uraniferous Humate Deposits, Grants Uranium Region, New Mexico. Final Report*; 1981; p GJBX-2(81), 6580071.

(28) Turner-Peterson, C. E. Fluvial Sedimentology of a Major Uranium-Bearing Sandstone—A Study of the Westwater Canyon Member of the Morrison Formation, San Juan Basin, New Mexico. In *A Basin Analysis Case Study: The Morrison Formation, Grants Uranium Region, New Mexico*; Turner-Peterson, C. E.; Santos, E. S.; Fishman, N. S., Eds.; American Association of Petroleum Geologists, 1986; Vol. *22*, pp 47−75.

https://doi.org/10.1021/acs.est.4c01257
Environ. Sci. Technol. 2024, 58, 15138−15146

(29) Browne, E.; Tuli, J. K. Nuclear Data Sheets for A = 60. *Nucl. Data Sheets* **2013**, *114*, 1849−2022.
(30) Khazov, Yu.; Rodionov, A.; Kondev, F. G. Nuclear Data Sheets for A = 133. *Nucl. Data Sheets* **2011**, *112*, 855−1113.
(31) Browne, E.; Tuli, J. K. Nuclear Data Sheets for A = 137. *Nucl. Data Sheets* **2007**, *108*, 2173−2318.
(32) Martin, M. J. Nuclear Data Sheets for A = 152. *Nucl. Data Sheets* **2013**, *114*, 1497−1847.
(33) Basunia, M. S. Nuclear Data Sheets for A = 176. *Nucl. Data Sheets* **2006**, *107*, 791−1026.
(34) Browne, E.; Tuli, J. K. Nuclear Data Sheets for A = 234. *Nucl. Data Sheets* **2007**, *108*, 681−772.
(35) Browne, E.; Tuli, J. K. Nuclear Data Sheets for A = 235. *Nucl. Data Sheets* **2014**, *122*, 205−292.
(36) Abusaleem, K. Nuclear Data Sheets for A = 228. *Nucl. Data Sheets* **2014**, *116*, 163−262.
(37) Alnour, I. A.; Wagiran, H.; Ibrahim, N.; Hamzah, S.; Siong, W. B.; Elias, M. S. New Approach for Calibration the Efficiency of HpGe Detectors. *AIP Conf. Proc.* **2014**, *1584*, 38−44.
(38) De Corte, F.; Umans, H.; Vandenberghe, D.; De Wispelaere, A.; Van den haute, P. Direct Gamma-Spectrometric Measurement of the ^{226}Ra 186.2 keV Line for Detecting ^{238}U/^{226}Ra Disequilibrium in Determining the Environmental Dose Rate for the Luminescence Dating of Sediments. *Appl. Radiat. Isot.* **2005**, *63*, 589−598.
(39) Papachristodoulou, C. A.; Assimakopoulos, P. A.; Patronis, N. E.; Ioannides, K. G. Use of HPGe γ-Ray Spectrometry to Assess the Isotopic Compositiion of Uranium in Soils. *J. Environ. Radioact.* **2003**, *64*, 195−203.
(40) Gilmore, G. R. *Practical Gamma-Ray Spectrometry*; John Wiley & Sons, Ltd, 2008
(41) Bourdon, B.; Turner, S.; Henderson, G. M.; Lundstrum, C. Introduction to U-series Geochemistry. *Rev. Mineral. Geochem.* **2003**, *52*, 1−21.
(42) Hakam, O. K.; Choukri, A.; Reyss, J.-L.; Lferde, M. Activities and Activity Ratios of U and Ra Radioisotopes in Drinking Wells, Springs and Tap Water Samples in Morocco. *Radiochim. Acta.* **2000**, *88*, 55−60.
(43) Granger, H. C.; Santos, E. S.; Dean, B. G.; Moore, F. B. Sandstone-Type Uranium Deposits at Ambrosia Lake, New Mexico; an Interim Report. *Econ. Geol.* **1961**, *56*, 1179−1210.
(44) Sharifironizi, M.; Szymanowski, J. E. S.; Sigmon, G. E.; Navrotsky, A.; Fein, J. B.; Burns, P. C. Thermodynamic Studies of Zippeite, a Uranyl Sulfate Common in Mine Wastes. *Chem. Geol.* **2016**, *447*, 54−58.
(45) Brugger, J.; Burns, P. C.; Meisser, N. Contribution to the Mineralogy of Acid Drainage of Uranium Minerals: Marecottite and the Zippeite-Group. *Am. Mineral.* **2003**, *88*, 676−685.
(46) Lahrouch, F.; Baptiste, B.; Dardenne, K.; Rothe, J.; Elkaim, E.; Descostes, M.; Gerard, M. Uranium Speciation Control by Uranyl Sulfate and Phosphate in Tailings Subject to a Sahelian Climate, Cominak, Niger. *Chemosphere* **2022**, *287*, 132139.
(47) Plášil, J.; Sejkora, J.; Škoda, R.; Škácha, P. The Recent Weathering of Uraninite from the Červená Vein, Jáchymov (Czech Republic): A Fingerprint of the Primary Mineralization Geochemistry onto the Alteration Association. *J. Geosci.* **2014**, 223−253.
(48) Langmuir, D.; Riese, A. C. The Thermodynamic Properties of Radium. *Geochim. Cosmochim. Acta* **1985**, *49*, 1593−1601.
(49) Brown, P. L.; Matyskin, A. V.; Ekberg, C. The Aqueous Chemistry of Radium. *Radiochim. Acta.* **2022**, *110*, 505−513.
(50) Kelly, R. P.; Moran, S. B. Seasonal Changes in Groundwater Input to a Well-mixed Estuary Estimated Using Radium Isotopes and Implications for Coastal Nutrient Budgets. *Limnol. Oceanogr.* **2002**, *47*, 1796−1807.
(51) Moore, W. S. Seasonal Distribution and Flux of Radium Isotopes on the Southeastern U.S. Continental Shelf. *J. Geophys. Res.* **2007**, *112*, C10013.
(52) Bacon, J. R.; Davidson, C. M. Is There a Future for Sequential Chemical Extraction? *Analyst* **2008**, *133*, 25−46.
(53) Davies, B. E. Loss-on-Ignition as an Estimate of Soil Organic Matter. *Soil Sci. Soc. Am. Proc.* **1974**, *38*, 150−151.
(54) Heiri, O.; Lotter, A. F.; Lemcke, G. Loss on Ignition as a Method for Estimating Organic and Carbonate Content in Sediments: Reproducibility and Comparability of Results. *J. Paleolimnol.* **2001**, *25*, 101−110.
(55) Nash, J. T. Uranium Deposits in the Jackpile Sandstone, New Mexico. *Econ. Geol.* **1968**, *63*, 737−750.
(56) Robert, H. Moench. *Geology and Uranium Deposits of the Laguna District, New Mexico*; Professional Paper 519 ; U.S Geological Survey, 1967.
(57) Hatcher, P. G.; Spiker, E. C.; Orem, W. H.; Romankiw, L. A.; Szeverenyi, N. M.; Maciel, G. E. *Organic Geochemical Studies of Uranium-Associated Organic Matter from the San Juan Basin: A New Approach Using Solid-State /Sup 13/C Nuclear Magnetic Resonance*; American Association of Petroleum Geologists: United States, 1986.

https://doi.org/10.1021/acs.est.4c01257
Environ. Sci. Technol. 2024, 58, 15138−15146